Isothermal Characteristics of a Rectangular Parallelepiped Sodium Heat Pipe

Joon Hong Boo*, Soo Yong Park

School of Aerospace and Mechanical Engineering, Hankuk Aviation University, 200-1, Hwajeon-dong, Deogyang-gu, Goyang-city, Gyeonggi-do 412-791, Korea

The isothermal characteristics of a rectangular parallelepiped sodium heat pipe were investigated for high-temperature applications. The heat pipes was made of stainless steel of which the dimension was 140 m(L) × 95m(W) × 46 m(H) and the thickness of the container was 5 mm. Both inner surfaces of evaporator and condenser were covered with screen meshes to help spread the liquid state working fluid. To provide additional path for the working fluid, a lattice structure covered with screen mesh wick was inserted in the heat pipe. The bottom surface of the heat pipe was heated by an electric heater and the top surface was cooled by circulating coolant. The concern in this study was to enhance the temperature uniformity at the bottom surface of the heat pipe while an uneven heat source up to 900 W was in contact. The temperature distribution over the bottom surface was monitored at more than twenty six locations. It was found that the operating performance of the sodium heat pipe was critically affected by the inner wall temperature of the condenser region where the working fluid may be changed to a solid phase unless the temperature was higher than its melting point. The maximum temperature difference across the bottom surface was observed to be 114℃ for 850 W thermal load and 100℃ coolant inlet temperature. The effects of fill charge ratio, coolant inlet temperature and operating temperature on thermal performance of heat pipe were analyzed and discussed.

Key Words : Sodium Heat Pipe, Liquid Metal, Rectangular Parallelepiped, Isothermal Characteristics, Thermal Performance, High Temperature Application

Nomenclature

T : Temperature (℃)
Q_{in} : Input thermal load (W)
ϕ : Fill charge ratio of working fluid (%)

Subscripts

bottom: Bottom side of heat pipe
c.i : Coolant inlet
c.o : Coolant outlet
c.s : Inner wall of the condenser
v : Vapor

* Corresponding Author,
E-mail : jhboo@hau.ac.kr
TEL : +82-2-300-0107; **FAX** : +82-2-3158-2191
School of Aerospace and Mechanical Engineering, Hankuk Aviation University, 200-1, Hwajeon-dong, Deogyang-gu, Goyang-city, Gyeonggi-do 412-791, Korea. (Manuscript **Received** November 5, 2004; **Revised** February 25, 2005)

1. Introduction

The liquid metal heat pipes (LMHP) for high-temperature range can be used in many industrial applications including isothermal high temperature heater, thermometric calibration tools, die casting and mold system, glass forming process, and solar power system (Brost and Groll, 1995; Rosenfeld and Ernst, 1997). In previous studies on LMHP's, heat transfer limit, operation characteristics, and compatibility were investigated and most of the research works were on cylindrical geometry (Faghri et al., 1991a: 1991b; Ponnappan and Chang, 1994; Jang, 1995; Moraga and Jacobson, 1987). In recent works,

however, various geometries were studied depending on special demand and applications.

Colwell (1990) and Colwell and Modlin (1992) conducted modeling of a LMHP to dissipate rapidly a high temperature heat which occurs near the stagnation point of the leading edge of a hypersonic or re-entry vehicle. Glass (1998) designed and developed 'D' shape LMHP which was made of Mo-Li for leading edge cooling of a hypersonic vehicle and verified a stable operation in the design temperature range.

Reid et al.(2001) and Martin and Salvail (2004) evaluated performance of cylindrical LMHP module which was designed to remove thermal power from the SAFE (Safe Affordable Fission Engine) core, and transfer it to an electrical power conversion system.

Ground-based hybrid Dish/Stirling solar power system was designed and tested by Laing et al.(1997). A thermophotovoltaic system using LMHP module to provide isothermal radiator surface in photons energy conversion system was considered by Ashcroft et al.(1999). Park and Boo (2002) conducted a fundamental experiment on a rectangular parallelepiped LMHP with varying thermal load and coolant temperature.

In this study, more intensive investigation was performed on smaller size rectangular parallelepiped shape LMHP considering applications in glass molding process or an isothermal high temperature heater. The temperature uniformity at the bottom surface and the effect of the design factors were investigated. Especially, the influence of internal wick structure, coolant inlet temperature, and fill charge ratio of the working fluid was discussed.

2. Experimental Setup and Procedure

The dimension of the heat pipe in this study was 140 mm(L) × 95 mm(W) × 46 mm(H). The container material was stainless steel 304 and working fluid was sodium. The side edges and inner corner of box were rounded with fillet. The outer radius of the fillet was 15 mm and thickness of the wall was 5 mm. The height of the inner space was 30 mm and the inner radius of the corner was 10 mm. Fig. 1 illustrates the container of the heat pipe and was designated as 'Type A'. In Type A, double layer wick of 50-mesh screen were attached to the inner wall surface and a cooling block with coolant flow path was covered as a top surface, which worked as the condenser part of the LMHP.

Figure 2 illustrates an improved model of the rectangular parallelepiped heat pipe. It had a lattice structure covered with screen mesh wick in addition to the basic structure of Type A. The heat pipe was designated as 'Type B'. The lattice structure with screen mesh provided additional paths for the working fluid return.

The working fluid charge amount was expressed in terms of the fill charge ratio, ϕ, as defined by the following equation.

$$\phi(\%) = \frac{\text{charged liquid volume}}{\text{total pore volume in the wick}} \times 100 \quad (1)$$

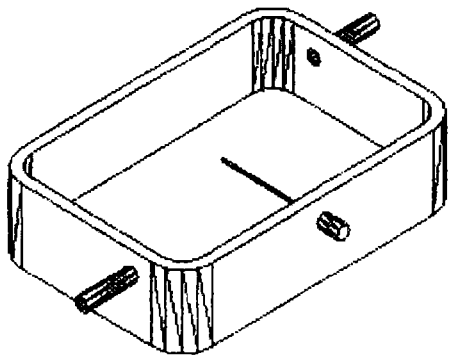

Fig. 1 Heat pipe container (Type A)

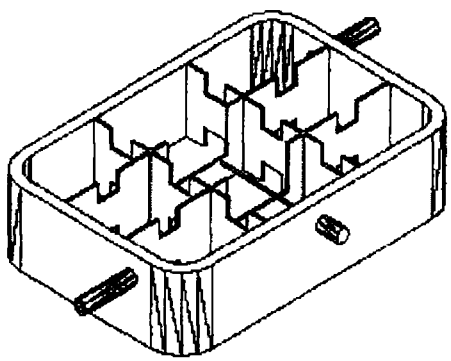

Fig. 2 Heat pipe with lattice structure (Type B)

Total pore volumes of heat pipe Type A and Type B were 14.8 cc and 25.9 cc, respectively, and these quantities correspond to the fill charge ratio 100% for each heat pipe since they had different wick structures.

The operation of the rectangular parallelepiped heat pipe is shown schematically in Fig. 3. The bottom surface of the heat pipe was heated by an electric heater and the top surface was cooled by circulating coolant. Vaporized working fluid from the bottom side moves to the top side and condense at the inner surface of the condenser. Then the condensed working fluid is distributed through the screen mesh wick due to capillary action. The condensed liquid returns to the bottom through the wick structure at the side wall being assisted by gravity. The energy transfer with the phase change is accompanied by the fluid circulation from the bottom to the top.

The heat source was an electric heater. Due to the alternating configuration of the ceramic board and heat coils, the heat flux of the heater was not uniform over the bottom surface.

Figure 4 shows the heater surface and the locations of the thermocouples at the bottom side of the heat pipe. Twenty-six thermocouples were attached at bottom side to measure the temperatures. Additionally, a probe thermocouple was inserted at the center of the vapor space to measure the operating temperature of the heat pipe (T_v). Another thermocouple was attached at the inner surface of the condenser which represented the lowest temperature of the working fluid ($T_{c,s}$) and served as a measure to judge if the sodium was either liquid or solid phase at the location. To monitor the inlet and outlet temperature of the coolant ($T_{c,i}$ and $T_{c,o}$), two thermocouples were inserted in the flow path of the coolant.

The schematic of the experimental setup is shown in Fig. 5. The heat pipe was insulated by ceramic fiber and vacuum chamber to minimize heat interaction with surroundings. All the thermocouples were connected with a data acquisition system and the whole set of the measured

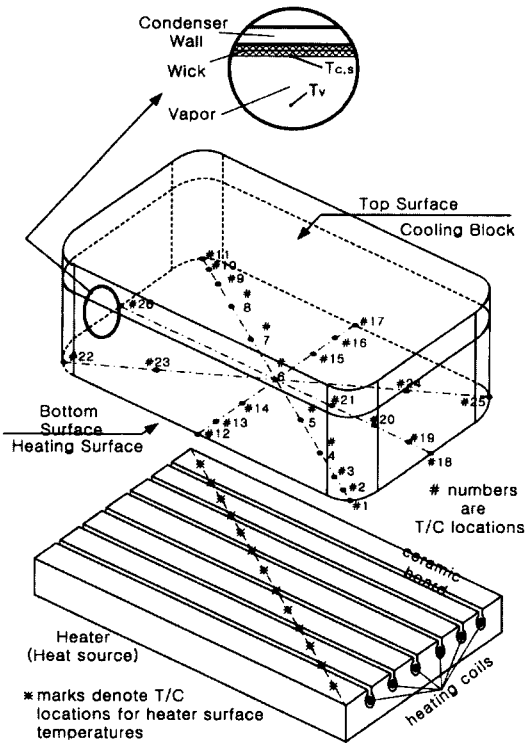

Fig. 4 Heat source and thermocouple locations

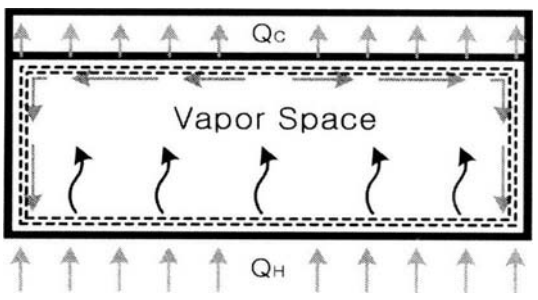

Fig. 3 Operation of the rectangular parallelepiped heat pipe (side view)

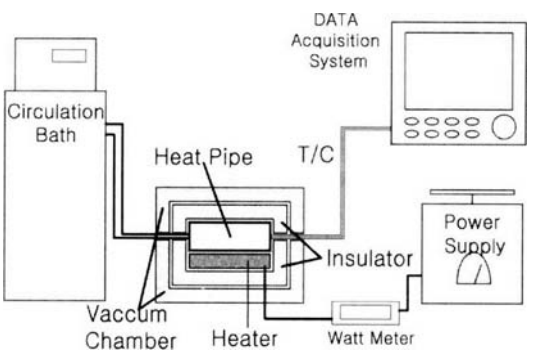

Fig. 5 Experimental setup

temperatures was recorded in every 10 seconds.

Fill charge ratio of each heat pipe was changed. For Type A, the fill charge ratios were 100%, 150%, and 200%. And for Type B, the fill charge ratios were 100%, 125%, and 150%. Coolant inlet temperature was controlled from 20℃ to 100℃ at 20℃ intervals. The thermal input for the heat pipe varied from 500 W to 900 W.

3. Results and Discussion

3.1 Type A — Simple wick model

Transient variation of temperatures at the bottom surface and other measuring points in the heat pipe was depicted in the Fig. 6 for fill charge ratios of 100, 150, and 200%. Fig. 6(a) is for the case when the fill charge ratio was 100%. For input thermal load of 500 W, the maximum temperature difference across the bottom surface was 213℃, and for input thermal load of 850 W, the temperature difference was 272℃. Although the coolant inlet temperature was increased up to 100℃, the difference was not improved. When the input thermal load and coolant inlet temperature were 850 W and 100℃, the temperature at the condenser inner surface ($T_{c,s}$) reached 240℃.

Figure 6(b) summarizes the temperature response of the heat pipe for fill charge ratio of 150%. The inlet temperature of the coolant was maintained at 100℃ and the input thermal load was increased from 500 W to 850 W. The maximum temperature difference observed was 151℃ for 500 W thermal load, and was 193℃ for 850 W thermal load. The maximum operating temperature of Type A was 650℃ and the temperature at the inner surface of condenser was 138℃.

Sufficient charge of working fluid was considered to enhance circulation of liquid in heat pipe. Fig. 6(c) summarizes temperature variation for 200%. When the time reached 120 minutes from start-up, the bottom surface temperature rapidly increased by a considerable scale and temperature difference was enlarged. When the coolant was supplied at 80℃, however, the temperature difference decreased very rapidly and the temperature of the condenser inner surface exceeded 98℃, which is a melting point of sodium. Apparently, normal operation for the heat pipe depends on the temperature at the condenser inner surface, $T_{c,s}$. When $T_{c,s}$ was lower than the melting point of working fluid, it was considered that condensed sodium was solidified at the inner surface of condenser. This caused an interruption of working fluid circulation and could result in operation failure. The first key to

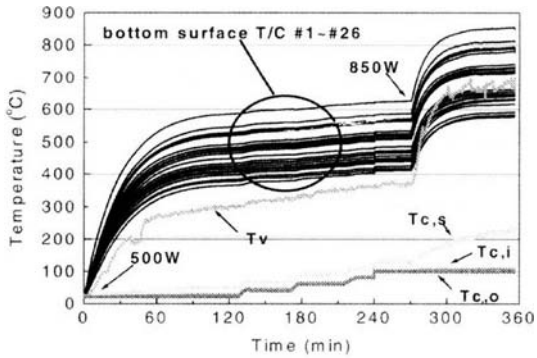

(a) ϕ=100%

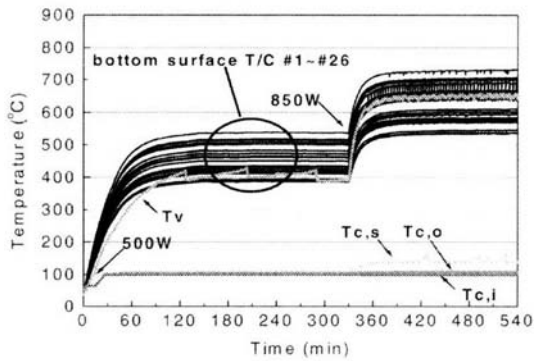

(b) ϕ=150%

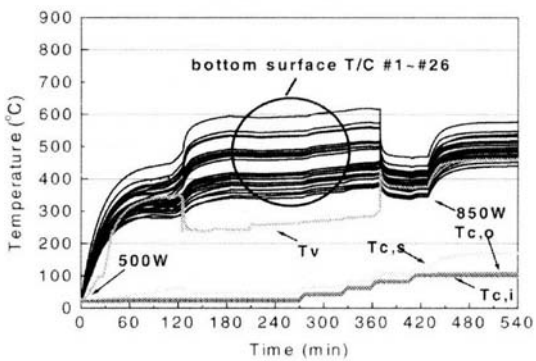

(c) ϕ=200%

Fig. 6 Transient temperature variation as a function of fill charge ratio of Type A heat pipe

avoid this failure is to maintain the condenser inner surface temperature above the melting point of the working fluid.

In this case, the maximum temperature difference at 850 W heat load was about 150℃, and it was smaller than those for lower fill charge ratios. Sufficient charge of working fluid could be considered to enhance circulation of working fluid.

Figure 7 shows temperature distribution at the heating side of the heat pipe when fill charge ratio was 200% and the coolant inlet temperatures were 20℃ and 100℃ for input thermal load of 850 W. In Fig. 7(a), the maximum temperature difference was 296℃ and the contour did not represent typical isothermal surface and the minimum temperature region appeared near the edges. The maximum temperature occurred at the center of the bottom the temperature contour of the simple plate heating without special cooling method. In Fig. 7(b), the maximum temperature difference across the bottom surface was observed to be 136℃, which was nearly a half of that appeared in Fig. 7(a). The result was similar to isothermal characteristic of heat pipes.

3.2 Type B — Lattice structure model

Figure 8 shows the temperature variation of

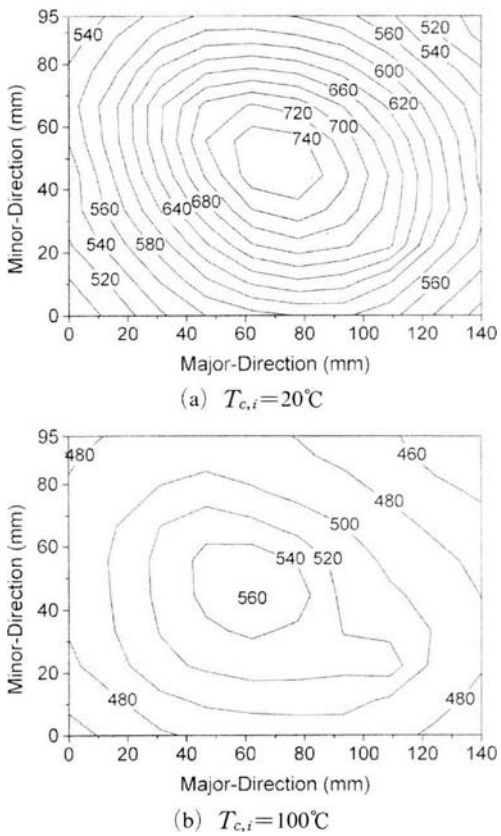

Fig. 7 Temperature distribution at the heating side of heat pipe. (Type A, ϕ=200%, Q_{in}=850 W)

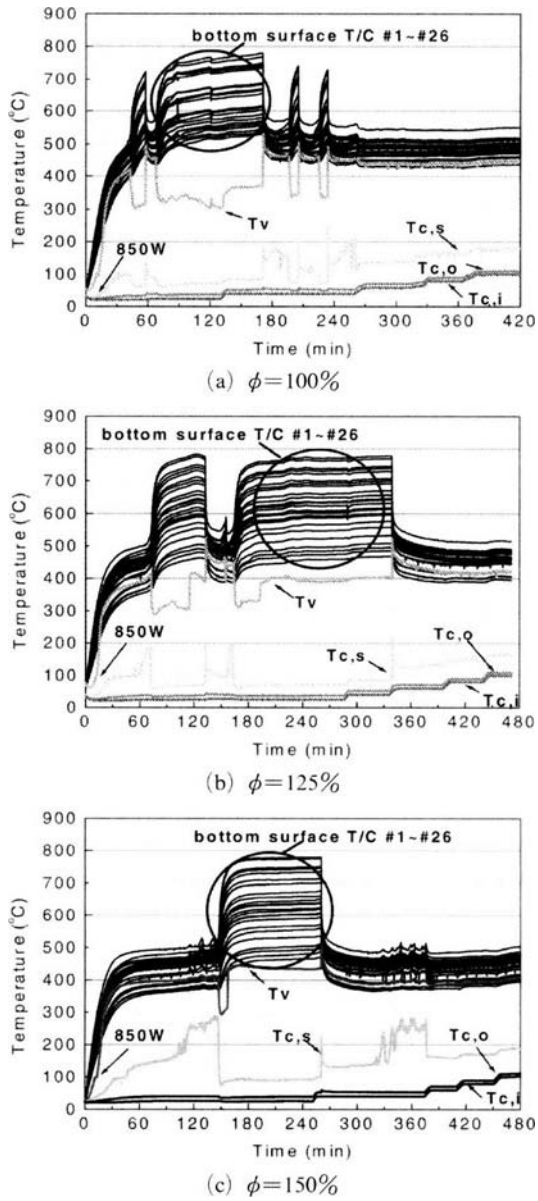

Fig. 8 Transient temperature variation as a function of fill charge ratio of Type B heat pipe

Type B model as a function of the coolant inlet temperature for three different fill charge ratios of 100, 125, and 150%. The input thermal load was 850 W and the coolant temperature was controlled. If the working fluid in the bottom wick was vaporized well enough by initial heat load, the bottom surface temperature would have been distributed with small temperature difference. After all the working fluid evaporated from the bottom wick, the bottom surface temperature increased and the operating temperature decreased rapidly. When the time reached 120, 160, and 150 minutes from start-up respectively, the temperature rising was observed in all case. It is considered that the increase of the coolant inlet temperature lowered the viscosity of the working fluid and helped the circulation of sodium. In Fig. 8(a), the fill charge ratio was 100%. It was started with 850 W heat load and temperature increased abruptly after 1 hour. The diverged and increased temperature values continued until $T_{c,s}$ was increased near 98℃ after 3 hours. As long as the condenser inner surface temperature was lower than melting point of sodium, similar problems occurred as we had for simple model. In this case, when the coolant inlet temperature was 60℃ at 4 hours and half, the heat pipe began its normal operation. And the temperature differences at bottom surface decreased considerably. At that time, the maximum temperature difference was observed to be 114℃.

In Fig. 8(b), 125% fill charge, a normal operation of the heat pipe began when the coolant inlet temperature was 60℃ and the maximum temperature difference was observed to be 120℃.

In Fig. 8(c), 150% fill charge, a normal operation began when the coolant inlet temperature was 40℃.

The result means that the variation of the charge of the working fluid allows the decrease of the coolant inlet temperature. In short, the lattice structure model showed normal operation with lower $T_{c,s}$ values than those for simple model. Increased quantity of working fluid partially condensed and circulated in the heat pipe with the aid of lattice structure inside.

Figure 9 shows the temperature distribution at the heating side of the heat pipe as a function of the coolant temperature for fill charge ratio of 125% and the thermal load of 850 W. The maximum temperature difference was 313℃ for the coolant inlet temperature of 20℃. However, when the coolant inlet temperature increased to 100℃, the maximum temperature difference decreased to 114℃. Increased coolant inlet temperature raised the temperature at the condenser inner surface. And the working fluid circulation was enhanced to reach a normal operation.

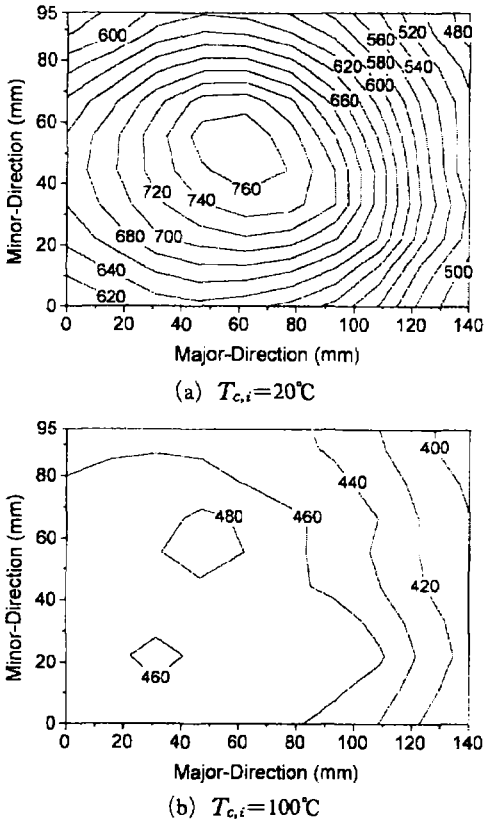

Fig. 9 Temperature distribution at the heating side of heat pipe. (Type B, ϕ=125%, Q_{in}=850 W)

Figure 10 shows the temperature distribution on the heater surface and the heating side of heat pipe in Fig. 9. To estimate the maximum temperature difference, the thermocouples were arranged diagonally on the heater surface and the heating side of heat pipe as shown in Fig. 4, and these points were projected to y-direction in Fig. 10. When the heat pipe was not operating normally,

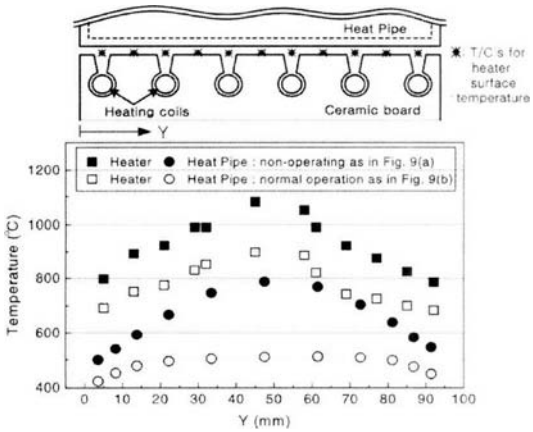

Fig. 10 Temperature distribution at the heater surface and the heating side of heat pipe in Fig. 9

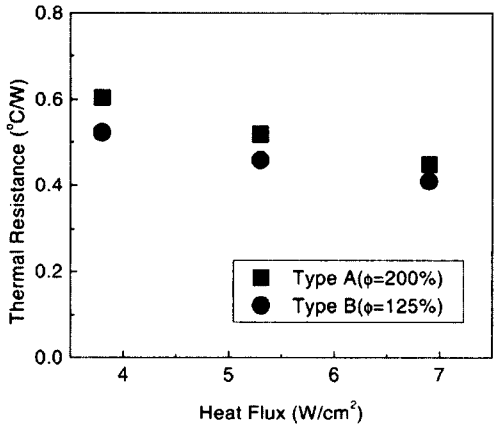

Fig. 11 Thermal resistance of LMHP

the maximum temperature itself and their maximum temperature difference on the heater surface were 1085℃ and 295℃, respectively, in a parabolic distribution. In this case, the maximum temperature difference on the heating side of heat pipe was 288℃, showing only a few degrees less than that on the heater surface. However, when the heat pipe was in normal operation, the maximum temperature itself and the maximum temperature difference on the heater surface decreased to 899℃ and 215℃, respectively. The maximum temperature difference on the heating side of the heat pipe in this case was 88℃, which showed a reduction by 127℃ from that on the heater surface. Through these examples, it may be stated that the heat pipe, when operating normally, reduced significantly the inherent temperature irregularity of heat source.

3.3 Thermal resistance

The results were compared from the viewpoint of thermal resistance as shown in Fig. 11. The values mean thermal resistance from the bottom to the inside wall of the condenser and were calculated using the following equation (2).

$$R_{HP}=\frac{\overline{T}_{bottom}-T_{c,s}}{Q_{in}} \quad (2)$$

where $\overline{T}_{bottom}$ is the average temperature across the bottom surface and $T_{c,s}$ is the inner surface wall temperature of the condenser. The heat flux was based on the bottom area (0.0131 m^2) and the input thermal loads, 500 W, 700 W, and 900 W. In order to compare the thermal resistance in the best performance, fill charge ratios of 200% and 125% are compared respectively. Such the charge ratio of the working fluid of Type A was larger than Type B, Type A had more quantity of the working fluid in the wick structure than that of Type B. The lower thermal resistance of the Type B was due to the thickness of the working fluid in the attached wick on the wall. In the tested heat flux range, the all values were above 0.4℃/W and showed decreasing trend as the thermal load increased.

4. Conclusions

Several conclusions can be stated on the isothermal characteristics of the bottom surface of a rectangular parallelepiped liquid metal heat pipe based on the observation of the effects of fill charge ratio of working fluid, input thermal load, and coolant inlet temperature.

(1) For normal operation of the liquid metal heat pipe, the temperature of the condenser inner surface (the lowest temperature in the heat pipe container) had to be maintained over the melting point of the working fluid to guarantee normal liquid return.

(2) Low coolant inlet temperature caused dif-

ficulty in working fluid circulation and hindered normal operation of the heat pipe. Additional charge of working fluid relieved this problem to some extent.

(3) The heat pipe with lattice structure operated in normal fashion with relatively lower fill charge ratio and coolant inlet temperature than those for the simple wick type heat pipe. The lattice structure was thought to have provided additional paths to enhance the return of working fluid and thus resulted in a better thermal performance. The number and size of the lattice cells have yet to be determined depending on the working conditions of specific applications.

References

Ashcroft, J. M., Merrigan, M. A., Bland, J. and Lindemuth, J., 1999, "Use of High Temperature Heat Pipes in Thermophotovoltaic Systems," *Proceedings of The 11th International Heat Pipe Conference*, Tokyo, Japan, pp. 213~218.

Brost, O. and Groll, M., 1995, "Liquid Metal Heat Pipe Applications: Thermometric Calibration Tools & Heat Transfer Components for Solar-Thermal Power Systems," *Proceedings of The 9th International Heat Pipe Conference*, Albuquerque, USA.

Cowell, G. T., 1990, "Cooling Hypersonic Vehicle Structures," *Proceedings of The 7th International Heat Pipe Conference*, Minsk, USSR, B-19.

Cowell, G. T. and Modlin, J. M., 1992, "Heat Pipe and Surface Mass Transfer Cooling of Hypersonic Vehicle Structures," *J. of Thermophysics and Heat Transfer*, Vol. 6, No. 3, pp. 492~499.

Faghri, A., Buchko, M. and Cao, Y., 1991, "A Study of High-Temperature Heat Pipes with Multiple Heat Sources and Sinks: Part I—Analysis of Continuum Transient and Steady Sate Experimental Data with Numerical Predictions," *ASME J. of Heat Transfer*, Vol. 113, No. 4, pp. 1003~1009.

Faghri, A., Buchko, M. and Cao, Y., 1991, "A Study of High-Temperature Heat Pipes with Multiple Heat Sources and Sinks: Part II—Analysis of Continuum Transient and Steady Sate Experimental Data with Numerical Predictions," *ASME J. of Heat Transfer*, Vol. 113, No. 4, pp. 1010~1016.

Glass, D. E., 1998, "Fabrication and Testing of a Leading-Edge-Shaped Heat Pipe," NASA/CR-1998-208720.

Jang, J. H., 1995, "Startup Characteristics of a Potassium Heat Pipe from the Frozen State," *J. of Thermophysics and Heat Transfer*, Vol. 9, No. 1, pp. 117~122.

Laing, D., Reusch, M. and Brost, O., 1997, "Hybrid Sodium Heat Pipe Receiver for Dish/Stirling System," *Proceedings of The 10th International Heat Pipe Conference*, Stuttgart, Germany, pp. 65~69.

Martin, J. and Salvail, P., 2004, "Sodium Heat Pipe Module Processing for the SAFE-100 Reactor Concept," *American Institute of Physics Conference Proceedings*, Vol. 699, pp. 869~874.

Moraga, N. O. and Jacobson, D. L., 1987, "Comparative Analysis of Sodium Heat Pipes," *Proceedings of The 6th International Heat Pipe Conference*, Grenoble, France, pp. 205~210.

Reid, R. S., Sena, J. T. and Martinez, A. L., 2001, "Sodium Heat Pipe Module Test for the SAFE-30 Reactor Prototype," *American Institute of Physics Conference Proceedings*, Vol. 552, pp. 148~155.

Rosenfeld, J. H. and Ernst, D. M., 1999, "Advances in Refractory Metal Heat Pipe Technology," *Proceedings of The 11th International Heat Pipe Conference*, Tokyo, Japan, pp. 245~251.

Park, S. Y., Boo, J. H. and Kim, J. B., 2002, "An Experimental Study on a Rectangular Parallelepiped Sodium Heat Pipe for High Temperature Glass Forming," *Transactions of the KSME (B)*, Vol. 26, No. 11, pp. 1622~1629.

Ponnappan, R. and Chang, W. S., 1994, "Startup Performance of a Liquid-Metal Heat Pipe in Near-Vacuum and Gas-Loaded Modes," *J. of Thermophysics and Heat Transfer*, Vol. 8, No. 1, pp. 164~171.